Investigations on forging of low-density Mg-Li alloys

Nikolaus Papenberg† Stefan Gneiger, Alexander Großalber, and Clemens Simson
LKR Light Metals Technologies Ranshofen GmbH
Lamprechtshausenerstraße 61, A-5282 Ranshofen, Austria
nikolaus.papenber@ait.ac.at – stefan.gneiger@ait.ac.at – alexander.grossalber@ait.ac.at – clemens.simson@ait.ac.at
† Corresponding Author

Abstract

Lightweight construction plays a vital role in aerospace applications and has a direct impact on fuel consumption and payload. Here, we present our investigations on a lightweight Mg-Li-Al-Ca-Y alloy. The material was produced through lab-scale casting and formed in a two-step forging operation. The manufacturing route and the processing behaviour are discussed, in addition the microstructure as well as the mechanical properties will be shown. In conclusion, we demonstrate the capabilities of Mg alloys with high Li contents, which are promising due to their remarkably low density and high specific mechanical properties.

1. Introduction

Light weighting is one of the most important topics in aeronautics and space applications, causing these industries to spearhead material innovation throughout the years. While a variety of new materials and composites have been used, structural parts made from light metals such as Al, Ti and Mg play a key role in aviation [1].

Among light metals, Mg holds a special place, as it is known to be the lightest structural metal in the world. Depending on the processing method used, its alloys can achieve specific mechanical properties comparable to those of high strength Al alloys. However, its limited ductility at medium and low temperatures, caused by its hexagonal (HCP) crystal structure, can lead to reservations regarding its processing and use. This can be mitigated by alloying with Li, which can greatly increase ductility by changing the brittle HPC crystal structure to the more ductile BCC structure, at additions above 10 wt. % Li. Furthermore, as the density of Li is only about 0.5 g cm^{-3}, the production of ultra-low-density alloys, 1.3–1.65 g cm^{-3} [2], can be realized.

A disadvantage of using Li is its high reactivity in most media, e.g. air, making production complicated and parts prone to oxidation. A discussion of the corrosion behaviour of Mg-Li alloys is difficult, as various types of oxide films can form on the material surface. Additionally, the change of the matrix crystal structure from α-HCP to β-BCC with rising Li content influences the interaction of matrix and oxide film. Nevertheless, in the case of two phase (BCC & HCP) as well as single phase (BCC) material, oxide films made from Li_2CO_3 have been reported to show good performance [2, 3].

Notwithstanding the chemical reactivity of these materials, the potential mass savings, making use of the exceptional specific strength and stiffness, as well as excellent forming behaviour further technical interest in Mg-Li alloys. Scientific investigations on Mg-Li alloys cover the full range of (i) single phase α-HCP [4], (ii) dual phase α-HCP & β-BCC as well as (iii) single phase β-BCC matrix alloys. Alloys with BCC crystal structure have attracted attention mainly because of the enhanced ductility at ambient temperatures, when compared to regular HCP Mg alloys. This improvement stems from the increased availability of independent slip systems caused by the change of the matrix crystal system: twelve in case of the BCC material (prismatic {110}<111> c+a slip) versus three in the original HCP structure (basal {0001} <11$\bar{2}$0> a slip) [5].

Investigations on the forming behaviour and material properties of BCC Mg-Li alloys processed by rolling [6, 7], extrusion [8] and multi directional forging [9] have been done. Overall, the focus lies on the Mg-Li-Al system [10], but other compositions have been reported as well, e.g. BCC Mg-Li-Zn alloys [7, 11].

It has been shown that also heat treatments play important role in material behavior and resulting mechanical properties. This has resulted in works reporting high (specific) mechanical properties of cast [11, 12] or wrought [7] Mg-Li alloys in combination with heat treatments, thereby reaching values of UTS > 450 MPa [12] and UCS > 500 MPa [11].

In this work we investigated the microstructure, oxidation behaviour and mechanical properties of a cast and forged Mg-20Li-15Al-1Ca-0.5Y alloy.

2. Material and Methods

2.1 Material

Aiming for an ultra-low-density alloy‡ (1.35 g cm⁻³) with good forming performance, as provided by the Mg-Li BCC crystal structure, an alloy with the chemical composition of Mg-20Li-15Al-1Ca-0.5Y (wt. %) was chosen, based on the well-studied Mg-Li-Al system. The alloying elements of Ca and Y are well known in the production of Mg alloys, providing (hardening) phases and reducing oxidation tendencies. For a better understanding of the phase formation within such an alloy, thermodynamic calculations‡ in equilibrium state are provided in Figure 1.

(a)   (b)
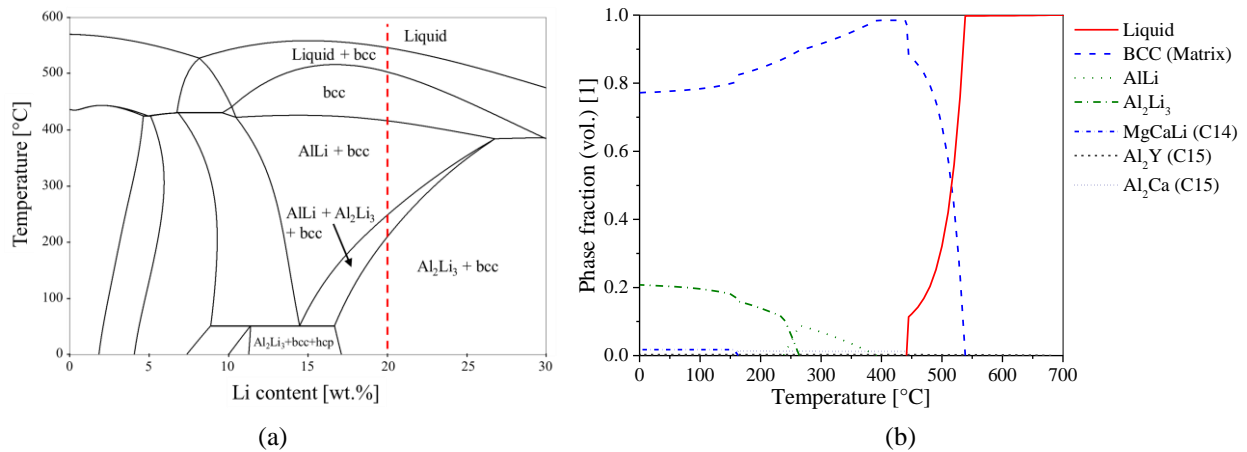
Figure 1: Thermodynamic calculations‡ of the Mg-Li-Al system given by (a) quasi-ternary phase diagram at 15 wt.% Al, actual alloy composition is indicated with a dashed line. The phase diagram of the alloy Mg-20Li-15Al-1Ca-0.5Y is shown in (b).
‡: CALPHAD calculations in equilibrium state have been done using Thermocalc TCMG6.

2.2 Methods

Casting of the Mg-20Li-15Al-1Ca-0.5Y (wt. %) alloy was done in a mild steel mould, producing billets with Ø 28 mm and a height of < 200 mm. The crucible was filled with the alloy components: Mg (99.95 %, ingot), Li (99.9 %, pellet), Al (99.9 %, granules), Ca (99.6 %, granules), MgY30 (Masteralloy, ingot) and subsequently processed in an induction heated furnace (Indutherm VC400 Generator F) with attached casting cell.

Flammability Testing of as-cast samples took place inside a pre-heated furnace (400, 425 and 450°C) at air. As-cast samples (Ø 22 × 10 mm) were placed on a pre-heated steel block inside the furnace chamber, as the thermic inertia of the steel block guaranties low temperature fluctuations during the measurement. Test duration was up to ~6 h, the sample temperature was measured by a thermocouple set into the sample centre.

Forging took place on a 250-tonne servo-hydraulic forming press (NEFF SDZP250), using a two-step forging die to produce parts in the shape of a piston rod. The cast round stock (Ø 22 × 90 mm) was formed isothermal at 180 °C, using a ram speed of 10 mm s⁻¹. Preheating was done in a forced convection chamber furnace (N120/85HA, Nabertherm GmbH) for 20 min, at air. To save stock material, only the inner section of the piston rods was used in the forming trials.

Microstructural Investigations were done on samples ground in isopropanol using up to 4000-grit SiC paper and subsequently polished with a diamond polishing suspension (Struers DP-Suspension-A, 1 µm). Analysis was performed using a field emission gun scanning electron microscope (SEM) of the type Tescan MIRA 3, equipped with a 4-quadrant solid-state backscattered electron (BSE) and an EDAX Octane Elect Super (EDS) detector. Images were recorded at 15 kV with a working distance of 10 and 15 mm for BSE and EDS analysis, respectively. Working distance of 20-25 mm was used for fracture surface investigations of tensile samples in secondary electron (SE) mode.

Mechanical Analysis consisted of tensile and compressive testing at room temperature (RT), using material in as-cast and as-forged state. Cylindrical samples ($\varnothing$ 4 × 8 mm) were used for compression testing, on a Bähr 805 A/D deformation dilatometer at 0.006 s^{-1}. Tensile testing was done on a Zwick (Z100) testing machine, according to DIN 50125, using round (A 8 × 40 mm) and flat (E 2.5 × 6 × 20 mm) samples for the as-cast and the as-forged material, respectively.

3. Results & Discussion

3.1 Process Analysis

Casting took place after pre-heating of the crucible and material for the duration of 0.5 h, using cover gas (Ar). The filled crucible was then heated to the casting temperature of ~800 °C and the melt mixed by electromagnetic stirring. Subsequently the melt was gravity cast into the mould and cooled at inert atmosphere. As the used processing temperature causes a loss of Li, the soaking and stirring time was kept short.

Flammability Testing was done to investigate the oxidation behaviour of the cast material. The sample temperatures measured during the testing are shown in Figure 2. The material tested at 450 °C immediately oxidized which led to an increase in temperature, subsequently igniting at ~500 °C. The material heated up to 425 °C repeatedly showed oxidation events after ~1 h, thereby reaching up to ~475 °C, without igniting. The testing of the sample at 400 °C showed only minor oxidation events and no significant heat gain during the full experiment duration of ~6 h. All investigated samples display grey and white oxidation products, while the sample tested at 450 °C fully disintegrated, see Figure 2.
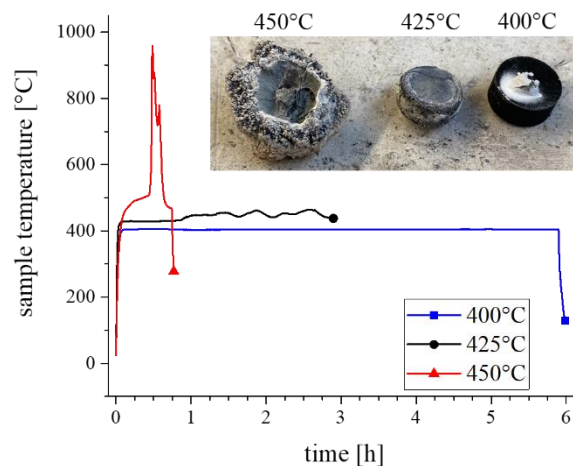
Figure 2: Results of flammability testing, showing the measured time-temperature curves and the samples the after finished experiments.

Closed Die Forging was used to produce parts in the shape of a piston rod, which allows the production of samples for tensile and compressive testing. The as-cast stock material was heated up to processing temperature (180 °C) and subsequently forged in the pre-heated forging die in two forging steps. The forming process took place within ~60 s, including the transition time of the material from furnace to the forging die. A graphite/water suspension was used for lubrication, the description of a comparable isothermal forging process can be found in [13].

The alloy showed good forming behaviour and well-formed parts were produced throughout. The flash showed minor cracks and underfillings are visible at the ends of the piston rod. These underfillings are of no consequence, as they are caused by the reduced stock material length, which is only intended to fully fill the inner section of the rod, see Figure 3.

(a)   (b)

Figure 3: Showing the used forging die, including the sequence of forging steps (a) and a forged part made from Mg-20Li-15Al-1Ca-0.5Y alloy (b).

3.2 Microstructural Investigations

As the used SEM/EDX detector is not capable of adequate detection and interpretation of Li content, the discussed microstructure was interpreted without the detection of Li. Nevertheless, a fairly well estimation of the presented microstructure can be done by the combination of well measurable alloying elements, i.e. Mg, Al, Ca, Y, and supporting CALPHAD calculations. The subsequently discussed microstructures of the as-cast and as-forged materials are shown in Figure 4.

The as-cast microstructure shows a Mg-Li matrix pervaded by large network-like structures of Al containing phases. This network is composed of at least two different phases, a fine lamellae Ca containing constituent, presumably Al_2Ca, and diffuse Al-rich phases without Ca. Furthermore, primary phases containing Y and Al with distinct blocky shapes and particle sizes of up to 10 µm can be found.

The forging process changed the microstructure mainly by dispersing the network-like structures of Al and Ca containing phases, thereby spreading the Al containing phases throughout the whole microstructure. The phases containing Ca on the other hand show banded structures of partially fractured particles. The phases containing Al and Y remain mostly unchanged.

The results from microstructural investigations coincides well with the CALPHAD calculations shown in Section 2. The Mg-Li matrix can contain varying amounts of Mg, Li and Al depending on material temperature. The amount of Li and Al are reduced with decreasing temperature, providing the elements necessary for phase formation of Al and Li containing phases, i.e. AlLi and Al_2Li_3. At RT, the matrix consists of solely ~60 at. % Mg and 40 at. % Li, while the Al is fully consumed by phase formation. The nearly homogeneous distribution of Al throughout the sample after the forging process is caused by the applied deformation but might also be enhanced by the processing temperature (180 °C), which is well within the formation range of Al_2Li_3. This phase consumes Li from the Mg-Li matrix and can amount to 20 vol. % of the microstructure. The Ca containing phases in the cast microstructure are assumed to be Al_2Ca (C15 structure), which forms in an eutectic reaction during solidification. At temperatures below 160 °C, this phase can change to a C14 Laves structured phase containing Mg, Ca and Li, as Al is gradually consumed by the formation of Al_2Li_3. However, no C14 Mg-Ca-Li phase was found in this microstructural analysis, coinciding with the processing temperature (180 °C) and the forgoing of a heat treatment at relevant temperatures.

(a)

(b)
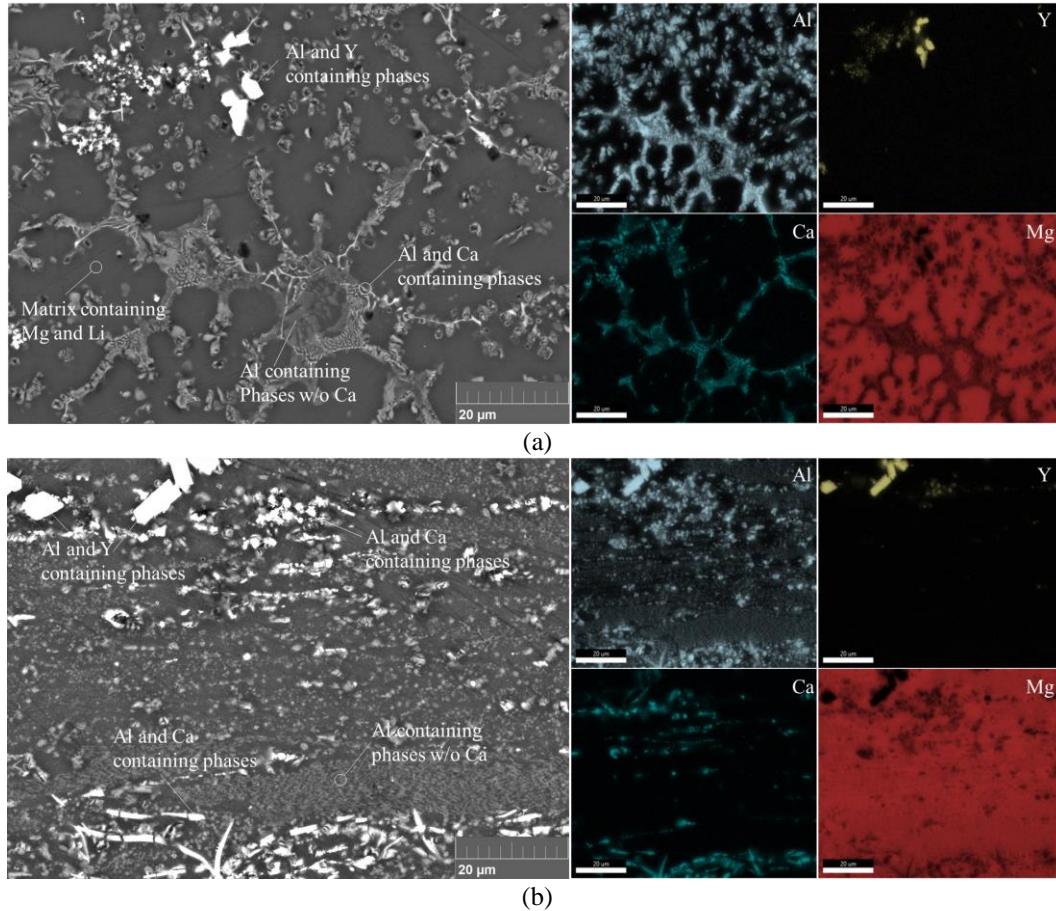
Figure 4: SEM/BSE micrographs of the (a) as-cast and (b) as-forged material. The EDS maps provided show the local content of measured Al, Ca, Y and Mg.

3.3 Mechanical Testing

Compressive Testing of the forged and cast samples showed nearly identical values, i.e. 300 MPa, for ultimate compressive strength (UCS). Nevertheless, the forming behaviour differs for both materials, with the forged samples reaching higher elongations and retaining higher strengths after UCS. A main issue of the tested samples is the scatter of strength and achievable strain, as visible in the cast samples. The results are given in Figure 5a, scatter is depicted via the enveloping stress-strain curves for both materials.

Tensile Testing provided distinct differences between cast and forged material, with samples made from the forged piston rods reaching better values throughout. The samples show a high scatter for both materials, well visible in the measured ultimate tensile strength (UTS) values. Especially the difference in elongation has a strong impact on the measured UTS values, as uniform elongation (ε_u) and elongation at break (ε_f) coincide in these measurements. Exemplary samples for of this test are shown in Figure 5b, the mean values are given in the insert.

While care must be taken when comparing the tensile properties measured with different sample geometries, the findings agree with the general deformation behaviour of the compressive samples. The forging operation disperses the large structures of intermetallic phases formed during casting and therefore increases mechanical properties markedly. This matches well with the large amount of (fractured) primary phases found on the fracture surface of a forged tensile sample. While brittle fracture of such alloys has been reported [10], the fracture surface of analysed tensile sample shows a ductile fracture with the characteristic microvoid formation around particles, see Figure 6.

The scatter measured in in both, the compressive and tensile samples, can be assumed to be a consequence of the casting process. To decrease loss of Li the holding and stirring time was kept short, thereby potentially reducing the melt homogeneity and increasing heterogeneous distribution of fracture inducing primary phases.

| (a) | (b) |
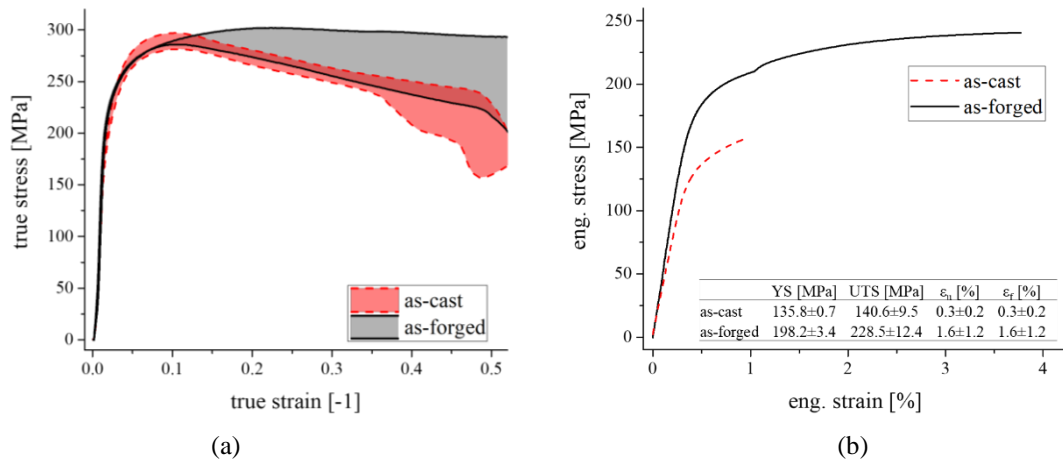
Figure 5: Results of mechanical testing, showing (a) the enveloping curves of compression testing, and (b) exemplary measurements from tensile testing, mean values including standard deviation are given in the inlay.

| (a) | (b) |
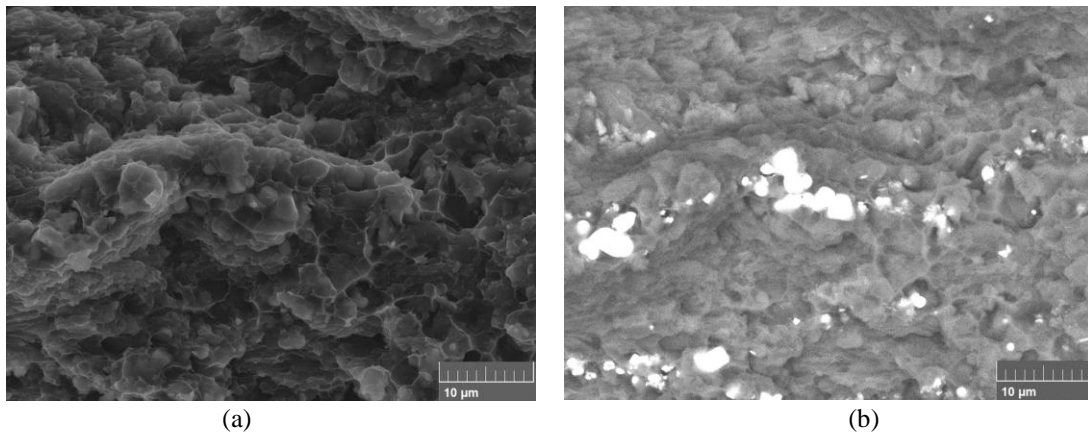
Figure 6: Fracture surface of as-forged tensile sample, showing (a) SEM/SE image of ductile fracture and (b) SEM/BSE micrograph with banded phase structures.

4. Conclusion

In this work an ultra-low-density Mg-20Li-15Al-1Ca-0.5Y alloy was investigated by isothermal forging. The following conclusions can be drawn:

- The flammability of the alloy was investigated at air and no major oxidation events have been detected during the six-hour testing period at 400 °C. Higher temperatures showed an increasing amount of oxidation events up to self-ignition at a soaking temperature of 450 °C.
- Isothermal forging took place at 180 °C, the material showed good forming behaviour and parts (shortened piston rods) were successfully produced in two forging steps.
- The forged samples showed an increase in strength and ductility when compared to the as-cast material in tensile testing. In the compression tests the strength of both materials was comparable, while lower ductility was measured in the as-cast samples.
- Microstructural analysis of cast samples, using SEM and EDS as well as CALPHAD calculations, showed a network-like structure of Al-Li and Al-Ca phases as well as blocky primary particles containing Y and Al. In the forged samples, larger phases were fractured and banded structures orthogonal to the forging direction are apparent.

While the investigated alloy showed promising forming behaviour, the addition of alloying elements, e.g. Zn [6, 7], and application of heat treatments, e.g. quenching [11, 12], can lead to improvements. Further insight in phase formation and Li distribution throughout the microstructure might be gained by new EDS equipment capable of evaluating the Li content [14], thereby creating new opportunities for the development of Mg-Li alloys.

Acknowledgements & Funding

References

[1] Zhang, S., and D. Zhao (Eds.). 2016. *Aerospace materials handbook.* CrC Press.

[2] Cain, T. W., and J. P. Labukas. 2020. The development of β phase Mg–Li alloys for ultralight corrosion resistant applications. *npj Mater. Degrad.*, 4, 17.

[3] Wang, B. J., Luan, J. Y., Xu, D. K., Sun, J., Li, C. Q., and E. H. Han. 2019. Research progress on the corrosion behavior of magnesium–lithium-based alloys: a review. *Acta Metall. Sin. (Engl. Lett.), 32, 1-9.*

[4] Haferkamp, H., Boehm, R., Holzkamp, U., Jaschik, C., Kaese, V., and M. Niemeyer, 2001. Alloy development, processing and applications in magnesium lithium alloys. *Mater. Trans., JIM*, 42(7), 1160-1166.

[5] Sun, Y., Zhang, F., Ren, J., and G. Song. 2023. Effect of Li Content on the Microstructure and Mechanical Properties of as-Homogenized Mg-Li-Al-Zn-Zr Alloys. *Alloys*, 2, 89-99.

[6] Ji, Q., Zhang, S., Wu, R., Jin, S., Zhang, J., and L. Hou. 2022. High strength BCC magnesium-Lithium alloy processed by cryogenic rolling and room temperature rolling and its strengthening mechanisms. *Mater. Charact.*, 187, 111869.

[7] Zhang, S., Du, C., Wu, R., Jia, H., Wu, Q., Zhang, J., and L. Hou. 2022. Insight into the increment of the formability and strength in bcc structured Mg–Li–Zn alloy. *Mater. Sci. Eng., A*, 850, 143563.

[8] Xin, T., Tang, S., Ji, F., Cui, L., He, B., Lin, X., Tian, X., Hou, H., Zhao, Y, and M. Ferry. 2022. Phase transformations in an ultralight BCC Mg alloy during anisothermal ageing. *Acta Mater.*, 239, 118248.

[9] Mineta, T., Hasegawa, K., and H. Sato. 2020. High strength and plastic deformability of Mg–Li–Al alloy with dual BCC phase produced by a combination of heat treatment and multi-directional forging in channel die. *Mater. Sci. Eng., A*, 773, 138867.

[10] Tang, S., Xin, T., Luo, T., Ji, F., Li, C., Feng, T., and S. Lan. 2022. Grain boundary decohesion in body-centered cubic Mg-Li-Al alloys. *J. Alloys Compd.*, 902, 163732.

[11] Zhang, S., Wu, R., Zhong, F., Ma, X., Wang, X., and Q. Wu. 2023. Ultra-high strength Mg-Li alloy with B2 particles and spinodal decomposition zones. *Fundam. Res.*, 3(3), 430-433.

[12] Xin, T., Zhao, Y., Mahjoub, R., Jiang, J., Yadav, A., Nomoto, K., Niu R., Tang S. Ji F., Quadir Z., Miskovic D., Daniels J., Xu W., Liao X., Chen L.-Q., Hagihara K., Li X., Ringer S., and M. Ferry. 2021. Ultrahigh specific strength in a magnesium alloy strengthened by spinodal decomposition. *Sci. Adv.*, 7, eabf3039.

[13] Papenberg, N. P., Arnoldt, A., Trink, B., Uggowitzer, P. J., and S. Pogatscher. 2022. Closed die forging of a Mg–Al–Ca–Mn–Zn lean alloy. *Mater. Sci. Eng., A*, 857, 144079.

[14] Österreicher, J. A., Simson, C., Großalber, A., Frank, S., and S. Gneiger. 2021. Spatial lithium quantification by backscattered electron microscopy coupled with energy-dispersive X-ray spectroscopy. *Scr. Mater.*, 194, 113664.